SAMPLING PROBE FOR INSTANTANEOUS MASS SPECTROMETRIC ANALYSIS OF RAREFIED HIGH ENTHALPY FLOW

R. E. Dix

ARO, Inc.

April 1969

PROPULSION WIND TUNNEL FACILITY

ARNOLD ENGINEERING DEVELOPMENT CENTER

AIR FORCE SYSTEMS COMMAND

ARNOLD AIR FORCE STATION, TENNESSEE

NOTICES

SAMPLING PROBE FOR INSTANTANEOUS
MASS SPECTROMETRIC ANALYSIS
OF RAREFIED HIGH ENTHALPY FLOW

R. E. Dix

ARO, Inc.

FOREWORD

The research reported herein was sponsored by the Arnold Engineering Development Center (AEDC), Air Force Systems Command (AFSC), Arnold Air Force Station, Tennessee, under Program Element 65701F, Project 4344, Task 02.

The results of research were obtained by ARO, Inc. (a subsidiary of Sverdrup & Parcel and Associates, Inc.), contract operator of AEDC, AFSC, under Contract F40600-69-C-0001. The research was conducted during the period from July 1, 1966, to June 30, 1967, under ARO Project No. PL3740, from July 1, 1967, to June 30, 1968, under ARO Project No. PL3840, and from July 1 to September 30, 1968, under ARO Project No. PL3912. The manuscript was submitted for publication on January 10, 1969.

This technical report has been reviewed and is approved.

Vincent L. Rocco
2nd Lt., USAF
Research Division
Directorate of Plans
   and Technology

Edward R. Feicht
Colonel, USAF
Director of Plans
   and Technology

ABSTRACT

An aerodynamically shaped probe has been developed for instantaneous mass spectrometric analyses of gas samples taken from low density, high enthalpy, hypersonic flows. The requisite 10^{-5} torr operating pressure for a quadrupole mass spectrometer mounted in the water-cooled probe was established and maintained by a liquid-hydrogen cryopump. During an initial series of 5-min tests, the detected composition of an arc-heated airflow with a stagnation condition of approximately 10 atm at 3000°K agreed well with a nonequilibrium flow expansion calculation.

CONTENTS

APPENDIXES

I. ILLUSTRATIONS

NOMENCLATURE

A_{cp}	Surface area of cryopump
A_o	Orifice area
C	Conductance of a vacuum connection
c	Specific heat of the cryodeposit
D	Diameter
k	Thermal conductivity of the cryodeposit
L	Length
ℓ	Latent heat of solidification
M	Molecular weight
$\dot{m}_o$	Mass flow rate of gas through sampling orifice
m/e	Mass-to-charge ratio

p	Pressure
$p_{g_{cp}}$	Pressure of the gas at the cryopump
p_s	Static pressure
p_o	Stagnation pressure
$\dot{q}_{cp}$	Heat flux per unit area of the cryopump
$\mathcal{R}$	Universal gas constant
R	Gas constant
Re	Reynolds number
S_{eff}	Effective pumping speed of a pump
S_{max}	Maximum pumping speed of a pump
S_p	Pumping speed of a pump
T_{cp}	Temperature of the cryopump
$T_{g_{cp}}$	Temperature of the gas at the cryopump
T_o	Stagnation temperature
T_s	Static temperature
T_{sat}	Saturation temperature of the gas
t	Time
t_c	Time available for effective cryopumping
V_{DC}	Direct-current component of voltage
V_o	Basic value of the r-f component of voltage
V_R	Total voltage supplied to quadrupole rods
V_∞	Free-stream velocity
$\dot{V}_{cp}$	Volume flow rate of gas to be cryopumped
y_c	A characteristic dimension
λ	Mean free path
μ	Gas viscosity
ρ_c	Density of the cryodeposit
$\rho_{g_{cp}}$	Density of the gas at the cryopump
ω	Frequency

SECTION I
INTRODUCTION

There are many experimental gas flows in which a direct measurement of chemical composition would be of great value. One of the most important of these is the rapid expansion of very high temperature air in a hyper-velocity wind tunnel nozzle. If such flows remain in equilibrium, even though the composition changes rapidly, the chemical and fluid dynamic behavior can be readily predicted theoretically and easily observed experimentally by taking a minimum number of flow measurements. In many cases of practical interest, however, the expansion is so rapid that the chemical reactions proceed more slowly than the flow changes, and equilibrium is not maintained. Theoretical and experimental analysis of non-equilibrium airflows is very complex because of the large number of degrees of freedom of the microscopic constituents that must be considered. The number of independent measurements that must be made to uniquely define the state of nonequilibrium flow is directly related to the number of degrees of freedom that are not in equilibrium. Most attempts to verify experimentally the theory of flow expansion with finite rate chemical reactions have relied almost exclusively on measurement of gross thermodynamic variables (Refs. 1 and 2). The agreement of such measurements with theoretical predictions has been accepted as powerful evidence that the finite rate theories are correct, but a complete and unambiguous verification requires that the chemical composition of the flows be determined as well.

It is impossible, without altering its composition, to remove and store for subsequent laboratory analysis a sample of a nonequilibrium gas flow. An accurate determination of the flow composition can be made only by an instantaneous analysis of the flowing gas, for which several techniques have been used. Probes have been developed which infer free-stream atom concentrations by measuring the difference in aerodynamic heat transfer to catalytic and noncatalytic probe surfaces. To date, only atomic oxygen (O) concentrations have been determined with these probes, and with accuracies of only 15 to 30 percent (Refs. 3 and 4). Other techniques include chemical titration measurements and measurements of optical absorption or optical emission (Ref. 5).

Recently, as part of a general study of flow diagnostics in arc-heated facilities, another approach has been investigated within the organization of the Propulsion Wind Tunnel (PWT) of the AEDC: instantaneous mass spectrometric analysis of the flowing gas. Commercial availability of small monopole and quadrupole mass spectrometers has made possible the fabrication of a sampling probe compact enough to operate in the

small-diameter core flows characteristic of low density wind tunnels, yet large enough to accommodate the mass analyzing device. The design and development of such a sampling probe to aid in the chemical calibration of an arc-heated low density wind tunnel is presented herein.

SECTION II
THE QUADRUPOLE MASS SPECTROMETER

2.1 GENERAL COMMENTS

In the sequence encountered by incoming particles, a mass spectrometer consists of an ionizer, in which a small fraction of flow particles is given a net charge, if required; a mass filtering or analyzing chamber, in which the charged particles are sorted by mass-to-charge ratio; and a charged particle detector. The descriptive term "quadrupole" applies, generically, to those mass spectrometers that accomplish mass separation with an electrostatic field of four poles, two positive and two negative. Four cylindrical rods serve as the poles, arranged with mutually parallel and appropriately spaced longitudinal axes. Figure 1, Appendix I, shows, schematically, the components of a typical quadrupole spectrometer. Diagonally opposite rods are electrically connected, creating two pairs of rods. These rod pairs have applied to them the equal positive and negative components, respectively, of the voltage waveform

$$V_R = V_{DC} + V_o \cos \omega t$$

As ions enter the quadrupole chamber on the central axis of the rod arrangement, the field established by the voltages $\pm V_R$ exerts forces on the ions that affect their trajectories through the chamber in a known manner dependent upon their mass-to-charge ratio, m/e. Therefore, at any instant, the trajectories of only those ions with the one proper m/e ratio pass through the ion detector entrance window. All ions with other m/e ratios experience trajectories that terminate on one of the rods. Then, as the d-c and r-f amplitudes vary through their allowable ranges with a constant amplitude ratio, the abundance of ions detected as a function of their m/e ratio is displayed on an appropriate instrument.

Additional theoretical discussion of the equations of motion of ions in the quadrupole field (Mathieu equations) is available in the literature, e.g., Refs. 6 through 8.

2.2 TEST INSTRUMENT DESCRIPTION

The particular quadrupole spectrometer used in the sampling probe described herein was a model of the Quad 200® series manufactured by Electronic Associates, Inc. It consisted of an axial beam ionizer (i. e., the ionizer was exposed to a sample particle beam, or flow, with an axis that coincided with the axis of the quadrupole array); the quadrupole filter, or analyzer; and an electron multiplier charged particle detector, arranged as in Fig. 1.

In operation, sample beam particles entered the Faraday cage, which was maintained at an adjustable positive potential with respect to ground (hereinafter called ion energy), wherein they were subjected to electron bombardment from the filament, having a potential (hereinafter identified as electron energy) maintained at a value below that of the Faraday cage. An electron extractor plate attracted electrons from the cage with a potential positive with respect to the cage. An ion "lens," consisting of the cage exit plate, a focus plate strongly negative with respect to ground, and a grounded plate, attracted the ions from the cage and focused them onto the central axis of the quadrupole array.

Once in the quadrupole field, the ions were sorted by mass-to-charge ratio, as described in Section 2.1, and as illustrated in Fig. 1. The ions that survived were accelerated toward the first dynode of the multiplier, which was operated at a highly negative potential. Upon impact with the dynode, each ion initiated an electron avalanche which produced at the collector an output current which was displayed on an oscilloscope.

Controls on the instrument console provided selective display of all or any portion of a mass range. The sweep time, or display time, for the desired range of m/e values could be set for from 50 msec to 30 min. It was also possible to continuously monitor the abundance of one value of m/e.

SECTION III
PROBE DESIGN CONSIDERATIONS

3.1 TEST FACILITY FLOW CONDITIONS

Both logic and prudence indicated that initial sampling studies be made in a facility in which rarefied flows of moderately high stagnation enthalpy could be established. Such a facility was available at the AEDC: an 18-in. low density wind tunnel operated in support of research in the PWT.

The 18-in. facility consists of a 250-kw arc heater; a 10-deg half-angle conical nozzle with several different fixed-diameter throat inserts and nozzle exit sections; an open-jet test section enclosed in a test chamber; a diffuser; a heat exchanger; and a six-stage steam ejector. An elevation of the facility is presented in Fig. 2, and a cross section of the test chamber is designated as Fig. 3.

For the design of the sampling probe, a stagnation condition of 20 atm and 3400°K was chosen, representing an actual condition established in previous tests in the facility. For these values of stagnation pressure and temperature, the nozzle exit conditions were as follows: static pressure, about 2.4×10^{-2} torr; static temperature, approximately 80°K; and static density, 1.08×10^{-4} amagats. The flow velocity was 2680 m/sec, with a Mach number of 14.85.

3.2 REQUIRED PROBE FUNCTIONS

To accurately determine the composition of the nozzle flow, it was, of course, necessary to admit to the mass spectrometer an undisturbed sample of the free stream. The first step in satisfying this requirement was to design the probe nose so that its shock wave would be attached to the lip of the sampling orifice. Further, the orifice itself had to be of sufficiently small diameter, compared to the mean free path of the flow, and negligible L/D to avoid collisional disturbance of the sample from wall effects.

Secondly, the static pressure within the probe had to be established and maintained at no more than 10^{-4} torr, preferably 10^{-6} torr, so that the mass spectrometer ionizer could function without arcing or premature filament burnout, and so that no recompression (and hence collisional disturbance) of the expanded sample would occur. It should be noted here that, for the accepted flow model of very early freezing of the severely expanded flows that exist in all such high enthalpy, low density facilities, further expansion of a flow sample into the probe interior would not substantially disturb the composition. It was required, then, to establish a pressure within the probe of about three to five orders of magnitude less than the free-stream static pressure of 2.4×10^{-2} torr.

It was also necessary to decide on the mode of operation: i.e., whether the probe was to sample intermittently or continuously. The rate at which the probe could be translated across the nozzle exit plane with the existing traversing mechanism determined the minimum expected duration of exposure of the probe to the flow (about 2 min). Since it was

4

probable that O-ring seals would be used, probe heating became a design factor. With the existing cooling water system, and assuming an expected cone-cylinder probe configuration, calculations based on the design flow conditions of Section 3.1 indicated that probe body temperatures would remain below the O-ring distortion temperature of 530°K for approximately 5 min.

Comparatively, data acquisition time was negligible and not a design factor, since a given range of m/e values could be displayed in as little as 50 msec, as discussed in Section 2.2.

In summary, the probe would be required to (1) admit a chemically undisturbed rarefied hypersonic flow sample to its interior by assuring an attached shock, (2) maintain an internal pressure of 10^{-6} to 10^{-4} torr, and (3) sustain no physical damage or distortion for sampling periods of at least 5 min.

SECTION IV
PROBE DESIGN PROCEDURE AND DESCRIPTION

4.1 OUTER CONFIGURATION

A cone was selected for the probe tip shape, with an included angle of 90 deg - blunt enough both to accommodate cooling water passages of reasonable size and to allow placing the quadrupole spectrometer head close to the sampling orifice, if required, yet sufficiently sharp to ensure attached shocks for a range of flow conditions. The quadrupole size and shape required, in addition, that the probe provide a cylindrical volume of approximately 7 cm in diameter and 30 cm long, mounted so that the cylindrical axis would be parallel to the free stream.

From previous empirical data, it was known that the test facility would operate without flow breakdown with cones of 60-deg included angle and base diameters of 10 cm injected after establishing the flow. With a probe diameter of about 7 cm, the proper area of the probe would therefore not exceed that of the largest model successfully tested, but its length would be considerably greater. Also, the strut on which the probe would be mounted would add more frontal area than the previous model strut. Hence, to allow testing of the probe at as many different flow conditions as possible, it was necessary to create a clean aerodynamic shape for the outer configuration, minimizing attachments, protuberances, or other appendages to the basic cone-cylinder shape envisioned.

4.2 PROBE PUMPING SYSTEM

Of course, only a very small fraction of those flow particles entering the probe would be analyzed by the spectrometer. The remainder, if allowed to accumulate, would serve only to increase the probe internal pressure. Since the quadrupole probe could operate only in a high vacuum, it was necessary to provide a means of preventing the accumulation of surplus particles.

To establish some form of vacuum pumping of the probe interior, the choices were (1) pumps located outside the nozzle flow and connected to the probe by appropriate lines, or (2) an internal, self-contained pumping system. Pumps attached to the probe and exposed to the nozzle flow were eliminated from consideration because of the blockage problem mentioned in Section 4.1.

Since the test chamber had a diameter of 2 m, to connect pumps outside its walls to the probe would have required lines about 1.5 m long. From Ref. 9, the free-molecular flow conductance, in liters/sec, of a long vacuum line with diameter and length given in centimeters, was

$$C \approx 12.1 \frac{D^3}{L} \tag{1}$$

Connecting a pump and a conductance in series results in an effective pumping speed of

$$\frac{1}{S_{eff}} = \frac{1}{S_p} + \frac{1}{C} \tag{2}$$

Hence, to maximize the effective pumping speed (i.e., to approach the pump speed), the conductance had to be maximized, which required either reducing the pump line length, or increasing the pump line diameter, with the latter having much the more efficient effect. Unfortunately, reducing the line length was virtually impossible, and increasing the line diameter aggravated the tunnel blockage problem. For example, assuming a reasonable and likely orifice diameter of 0.02 cm, an approximate computation revealed a required effective pumping speed of 850 liters/sec to maintain a probe pressure of 10^{-6} torr. From Eq. (1), to provide a conductance of 850 liters/sec in a pumping line 1.5 m long would require a line diameter of 22 cm, far beyond reason.

After these fundamental observations, attention shifted to selecting a pumping system that could be mounted within the probe envelope. Successful experience with liquid hydrogen (LH_2) cryopumping (Refs. 10 and 11), and the availability of bulk and local storage facilities, transfer equipment, and trained personnel all suggested its use. The final decision to use LH_2 cryopumping was based not only on these "convenience"

factors, but also on estimations of required cryosurface area and available pumping time, as discussed in Appendix II.

Since all other considerations indicated that the probe would be cylindrical, an open-end, annular, right-cylindrical shape was chosen for the cryopump. The probe orifice diameter and the cryopump outside and inside diameters and length were taken as variables of the following iteration: an orifice diameter was chosen, thereby fixing the cryosurface area, which was then matched with some combination of cryopump dimensions. If a suitable combination of dimensions could not be selected, a new orifice diameter was chosen.

4.3 PROBE ORIFICE

The function of the orifice was, of course, to limit the mass flow into the probe without disturbing the free-stream composition. As noted in Section 3.2, it was necessary to maintain the probe internal pressure at 10^{-6} to 10^{-4} torr for about 5 min. As a first approach to selection of an orifice diameter, a value near the free-stream mean free path was selected. The mean free path at the design flow condition was computed from

$$\lambda = \frac{16}{5\sqrt{2\pi}} \frac{\mu}{P} \sqrt{RT} \tag{3}$$

taken from Ref. 12. The value obtained was 0.036 cm. This value of orifice diameter was used to begin the iterative procedure defined in Section 4.2. The final value of 0.0254 cm was chosen after several iterations and consultation with machine shop personnel concerning their fabrication facilities.

4.4 FINAL CRYOPUMP CONFIGURATION

After accepting a probe orifice diameter, the probe cryopump size was determined, as discussed in Appendix II. The necessary surface area was approximately 140 cm^2. To allow insertion of the quadrupole ionizer into the cryopump, an inside diameter of the annular cylinder of 4.5 cm was required, and to restrict the probe diameter to about 7 cm, the cylinder outside diameter was limited to 6 cm. A length of 10 cm was then necessary to provide the requisite cryosurface area. The final cryopump area exposed to the incoming flow was approximately 140 cm^2, as required. The remainder of the cryosurface (outside diameter) was to serve as a pump for maintaining a low background pressure in the probe.

4.5 FINAL PROBE CONFIGURATION

Figure 4 is a section view of the test chamber, showing the probe, its docked position, and a typical test position. Figure 5 is a section view of the completed probe.

Connections for ionizer voltages, rod voltages, and electron multiplier high voltage and output current were established between the quadrupole in the probe and the control console outside the test chamber by appropriate electrical cables and vacuum feedthroughs. A metal tube was attached to the rear of the probe for protective routing of some of the cables (see Section 6.3).

A water-cooled strut provided means for attaching the probe to the traversing mechanism and allowed cooling water, cryofluid transfer lines, and roughing vacuum line connections to be made outside the nozzle flow. Demineralized cooling water was supplied by a 400-psi source.

SECTION V
PROBE CALIBRATIONS

5.1 HEAT-TRANSFER CALIBRATION

After the probe body and support strut were fabricated, they were installed in the test facility for evaluation of flow blockage and the cooling water system. For this test, the quadrupole head was not mounted within the probe. Thermocouples were attached at points on the probe corresponding to O-ring locations.

Figure 6 contains the results of the heat-transfer calibration. A flow with stagnation conditions of $p_o \approx 5$ atm and $T_o \approx 3680°K$ was established, into which the probe was injected with the traversing mechanism. Thermocouple readings were obtained for about 5 min, after which the probe was extracted from the flow. The arc was extinguished and the probe allowed to cool for some 3 min. The arc was reignited, and flow with a stagnation pressure and temperature of approximately 19 atm and 3510°K, respectively, was established. The probe was reinjected, and again thermocouple data were recorded for nearly 5 min - this time until the hottest thermocouple reached 475°K, near the O-ring distortion temperature.

After the test, an inspection of the probe revealed no damage or distortion. Hence, it was concluded for reservoir pressures greater

than 5 atm, and for reservoir temperatures less than 3700°K, that flow blockage would not occur, and that the cooling water system was adequate for the design exposure period of approximately 5 min.

5.2 INTERNAL PRESSURE CALIBRATION

To measure the pumping capacity of the cryopump and the ultimate pressure attainable in the probe, the probe was mounted in a high vacuum chamber with LH_2 service lines. The probe cryopump was filled with LH_2, and gas from a supply outside the chamber was allowed to leak into the probe orifice from a small plenum chamber attached to the conical tip of the probe. Mass flows into the probe corresponding to those to be sampled in the 18-in. wind tunnel were established, and internal probe pressure recorded for from 20 min to 1 hr. An ionization gage used to sense the probe pressure was attached to the downstream end of the probe in place of the electrical feedthrough.

Before conducting the probe pressure history tests, an attempt was made to identify the basic species of the leak gas. Two purposes were intended: (1) checking the operation of the instrument in the probe, and (2) investigating the function of the internal, second orifice mounted upstream of the ionizer (Fig. 5). With a 0.0254-cm-diam orifice in place, no species were detected for 20 min, despite a steady leak into the probe from a supply of air at approximately 1 torr. A helium (He) leak was connected to the plenum so that operation of the instrument could be confirmed. Immediately, a peak corresponding to $m/e = 4$ was observed, verifying proper functioning of the quadrupole. Then, after about 30 min, peaks at $m/e = 1, 2, 4, 20, 21,$ and 22 were observed, corresponding to H, H_2, He, and the neon family Ne^{20}, Ne^{21}, and Ne^{22}. The second orifice was replaced with one of 0.254-cm diameter, and the leak test repeated. Species were detected immediately at $m/e = 18, 28,$ and 32, corresponding to water (H_2O), nitrogen (N_2), and oxygen (O_2). The second orifice was then removed, and a third leak test conducted, during which the peaks 18, 28, and 32 were again immediately detected.

The quadrupole electrical feedthrough at the downstream end of the probe was replaced with an ionization gage tube, and the leak test sequence repeated. The results are presented in Fig. 7. Although various vacua were established before initiating the leak, the presence of the second orifice apparently made little difference in the subsequent pressure history sensed by the ionization gage tube. However, an unexpected steady decrease in probe pressure with leak time was observed - as if the leak had not existed. The entire quadrupole head was then removed, leaving, therefore, no blockage between the ionization gage tube and the

orifice, and the leak test repeated. The pressure history sensed by the ionization gage tube then indicated the expected increase with leak time. This behavior was interpreted as a verification that the mean free path of the rarefied environment established by the cryopump upstream of the quadrupole head was greater than the annular clearance between the quadrupole and the cryopump, i.e., approximately 0.4 cm. Hence, the pressure upstream of the quadrupole head must have been no more than approximately 10^{-3} torr, the pressure of the test gas at which $\lambda = 0.4$ cm. Although this observation was not definitive, it was in agreement with the pressures measured and stated in Fig. 7.

The results of the pressure calibration were recognized to be only approximate, at best, since the leak gas was merely ambient air, not, of course, simulating temperature or velocity effects of the actual nozzle flow to be sampled. Two conclusions were made, however: (1) the pressure at the ionizer could not be accurately predicted empirically, and (2) for the design test time of 5 min, significant rarefaction of the sampled flow would be provided, probably sufficient to reduce particle collisions to a negligible number before entering the ionizer.

SECTION VI
OPERATIONAL COMPLICATIONS

6.1 CRYOFLUID LINE LEAKS

During fabrication of the probe, tests for leaks under vacuum conditions were performed as components were completed. These leak checks typically involved attaching the completed component to a helium leak detector. Unfortunately, all such leak checks were performed at atmospheric temperature, not cryogenic temperatures. Therefore, components that would contain the LH_2 cryofluid were not leak checked at their intended use temperature. A partial test of these components containing cryofluid was conducted by placing them in a vacuum chamber and introducing liquid nitrogen (LN_2). Then, with appropriate instruments, the chamber pressure was monitored for changes. For all components tested in this manner, the vacuum surrounding the component did not deteriorate, and when the LN_2 was forced out of the components with helium, the leak detector sampling the vacuum chamber did not indicate a leak.

After completion, the probe was installed in the high vacuum chamber mentioned in Section 5.2 for a check of the LH_2 system. When LH_2 was introduced, a rapid deterioration of the probe vacuum occurred. Investigation indicated that welds which had apparently been vacuum tight

at both atmospheric and LN_2 temperatures had failed at LH_2 temperature. When the probe was brought to atmospheric temperature and pressure, however, these "cold" leaks could not be detected. Only by forcing the LH_2 from the probe under vacuum with helium would a cold leak be detected. Although it was established that the leaks existed at the top of the probe strut in the vicinity of the LH_2 line penetrations, they could not be accurately located, and attempts to reweld suspected joints failed. A major redesign and subsequent refabrication of the probe strut was accomplished, in which welds of thin-wall tubing to much thicker pieces were eliminated. The modified strut is shown in Fig. 5.

6.2 COOLING WATER LINE RUPTURE

During pumpdown for the fifth test attempt in the 18-in. wind tunnel, a silver-soldered coupling in one of the cooling water lines to the probe nose failed, filling the probe with demineralized water. Investigation revealed that it was possible that the failure had occurred near the end of the fourth test. That test had been conducted without the arc heater, hence no cooling water flow had been required. It was possible that the stagnant water trapped in the nose cone and its lines from previous tests had frozen during the test run, applying extreme pressure on the soldered coupling joint, possibly cracking it. Then, when the water flow was established for the next run, complete failure could have occurred, causing the probe to fill with water. Another possible explanation was simple fatigue of the joint attributable to pressure cycling from 0 to 400 psig.

The leak was corrected by removing the water lines and replacing them with new, one-piece lines having no soldered couplings. The original configuration is shown in Fig. 5.

Freezing was still a possibility, since the water lines cleared the LH_2 cryopump by less than 0.5 cm; therefore, a procedure was established in which the lines would be emptied, upon termination of the water flow, by forcing air through them.

6.3 HIGH VOLTAGE ARCING

The electron multiplier (Figs. 1 and 5) required a 3000 vdc supply negative with respect to ground, which was brought first from the control console into the test chamber and then into the probe by coaxial cables using hermetic high voltage feedthroughs. At both the test chamber wall and the probe feedthrough flange, arcing of the high voltage conductor to ground within the connectors occurred during runs in which the test

chamber static pressure was about 5×10^{-2} torr. A separate test series with these connectors indicated that for the leakage path to ground which they provided, 3000 vdc could be carried only at pressures less than 4.5×10^{-2} torr or greater than 50 torr. Since static pressures in the tunnel were frequently in this forbidden range, and since it was virtually impossible to change connectors, it was necessary to provide a means of changing the pressure at the connectors. A flexible stainless steel bellows-type tube was therefore installed, connecting the feedthrough flange on the downstream end of the probe with a port at the chamber wall. The high voltage cables then passed, at atmospheric pressure, directly from the control console to the probe feedthrough, thereby eliminating the arcing. The tube served as well to protect the cables from overheating, which had also been a problem. (Figures 4 and 5 indicate the tube location.)

SECTION VII
INITIAL SAMPLING EXPERIENCE

7.1 TEST PROCEDURE

Between test runs, the aft section of the sampling probe, in which the quadrupole head was mounted, was kept under vacuum by attaching it to a storage chamber, a small separate vacuum system designed for the purpose. Preparation for a sampling test in the 18-in. wind tunnel began by removing the aft section of the probe from the storage chamber and attaching it to the forward section of the probe in the test chamber. The cables were connected to their feedthroughs at the probe, the cable tube was attached, and the test chamber was closed.

With the probe in its docked position, as in Fig. 4, a cap was moved into place to seal the probe orifice before sampling. This sealing cap was translated by the piston of a hydraulic system having an actuator that was mounted outside the test chamber. Thus sealed, the probe was evacuated to a rough vacuum of approximately 2×10^{-2} torr by a mechanical vacuum pump also located outside the chamber and connected to the probe by a 1.2-cm-diam line.

With both the test chamber and the probe evacuated to rough vacua, the probe cooling water was turned on, and the LH_2 cryopump filled. A flow of air to the arc heater was established, and the arc ignited. When the desired stagnation conditions had been stabilized in the arc chamber, the sealing cap was retracted and the probe traversed to the selected station in the flow.

After sampling, the probe was moved back to its docked position at the top centerline of the nozzle exit, the sealing cap was again moved into place, and the nozzle flow terminated. When the test chamber was opened, the aft section of the probe was detached from the forward (cryopump) section and again connected to the separate storage chamber for evacuation.

7.2 INITIAL RESULTS

For the initial sampling studies, a stagnation condition of 10 atm and 3000°K was chosen. This condition, according to the nonequilibrium nozzle flow expansions described in Ref. 2, would provide a test environment at the nozzle exit that contained negligibly small abundances of most ionized and atomic species, yet which would be sufficiently hostile to check the probe cooling and pumping systems. A series of nine tests was conducted at this stagnation condition.

In the first test, the probe was exposed to the flow for about 4.5 min. Four photographs were made of the spectrometer output signal displayed on an oscilloscope. Figure 8a shows the abundance (ordinate) of the detectable species for the mass range $m/e = 1$ to 48 (abscissa) after an exposure of approximately 2 min. (Species were detectable as soon as the probe entered the boundary layer of the nozzle flow, although no photographs were made until the probe reached the nozzle centerline, i.e., about 45 sec.) The prominent identifiable peaks at $m/e = 28$, 30, and 32 correspond to N_2, NO (nitric oxide), and O_2, respectively. For these tests, the electron energy was set at 30 v, only one-third of the maximum energy available with the control circuit furnished by the manufacturer. A separate series of tests had indicated that 30 v would not cause detectable dissociation within the ionizer itself.

The most abundant of the various nitrogen-oxygen species was apparently NO, a completely unexpected result. The composition inferred from Ref. 2 included, for the test flow condition, an O_2 abundance of 0.233 relative to that of N_2, and 0.0591 for the ratio $NO:N_2$, but from the test data, of which Fig. 8a was representative, the ratios were $O_2:N_2 \approx 0.26$, and $NO:N_2 \approx 6.4$. The $O_2:N_2$ ratio was in reasonable agreement with theory, but the $NO:N_2$ ratio was not. Also, since four sweeps of the mass range were made during the exposure time of the photograph, it was apparent that the peak shapes for N_2 and O_2 were smooth and steady, but the peak of NO was irregular and unsteady.

As the probe was withdrawn from the flow, the irregularities in the NO peak vanished, as shown in Fig. 8b. The presence of a prominent peak at $m/e = 18$, corresponding to water vapor, prevented the

acquisition of quantitative data from this photograph, since such was considered evidence that a degradation in capture coefficient, and hence pumping speed, of the probe cryopump was occurring. However, it was obvious that as the boundary layer was traversed, the peak instabilities gradually diminished from large values throughout the core flow to zero at the nozzle wall, where all peaks were stable and much nearer their correct ratios.

A test was then conducted during which the abundance of the NO peak alone as a function of time was displayed on the oscilloscope (Fig. 9). The very irregular abundance recorded confirmed the existence of random and short duration (about 1 msec) bursts of detected particles at $m/e = 30$. Since there was no evidence to support an argument of abnormal instrument function, it was thought probable that free-stream ions were the cause of the irregular peaks.

To detect free-stream ions, it was necessary to eliminate the instrument ionizing function but retain the focusing and filtering action. To this end, the control circuitry was modified to provide for disabling the filament and to allow operation of the Faraday cage at any potential up to a somewhat arbitrarily chosen 300 v with respect to ground. With no electron emission from the filament, i.e., with no ionization within the instrument, an output signal could be attributed to free-stream ions. Then, if the free-stream ion signal could be eliminated by increasing the cage potential, further substantiation of their existence would be made. In fact, a rudimentary estimate of their energy could be made, since only ions sufficiently energetic to overcome the repulsion of the cage potential could pass through the ionizer, thereby reaching the quadrupole section and finally the electron multiplier.

With the filament disabled and zero cage voltage, all peaks vanished except $m/e = 30$ and 40, corresponding to NO^+ and A^+ (argon), respectively (Fig. 10). As the cage voltage was increased, the height of both peaks decreased until they were no longer detectable. The A^+ peak vanished at approximately 10 v, but the NO^+ peak persisted until 105 v. This behavior was interpreted as irrefutable evidence that NO^+ ions existed in the free stream, probably created by the arc process. It should be noted here that the overabundance of NO^+ relative to N_2 indicated in Fig. 8a could not be accepted prima facie as evidence of a preponderant free-stream abundance of NO^+. At least two equipment characteristics contributed to the detected NO^+ signal: an unnatural attraction of charged particles to the grounded probe, and the fact that many more, if not all, of the free-stream ions would be detected, whereas normally only a small fraction of the neutral particle population is ionized and detected. Hence, with no calibration of the instrument sensitivity to ions, no comparative analysis of the indicated free-stream NO^+ and N_2 abundances could be made.

At the cage voltage for which all NO^+ had been repelled, the spectrum, with filament on, appeared as in Fig. 11. Unfortunately, at the time of the exposure of Fig. 11, alterations in the circuitry had not been made to maintain an electron energy of 30 v. It was later determined that the electron energy was effectively 135 v, far in excess of the bond dissociation energies of N_2 (9.75 ev) and O_2 (5.1 ev) given in Ref. 13. Therefore, dissociation of N_2 and O_2 within the ionizer was inferred, accounting for the detection of N and O atoms at m/e = 14 and 16, and the OH radical at m/e = 17. Also detected was the ubiquitous H_2O at m/e = 18, and A at m/e = 40. Ignoring the dissociated species produced in the ionizer, the comparison of fractional abundances with those derived from the finite-rate expansion program described in Ref. 2 is as follows:

Specie	Finite Rate Calculation	On-Line Sample by Mass Spectrometer
N	Negligible	---
O	0.014	---
N_2	0.763	0.793
NO	0.045	0.041
O_2	0.178	0.151
A	---	0.015

A later test with the electron energy correctly adjusted to 30 v verified that it was possible to repel the NO^+ ions without dissociating N_2 and O_2. Figure 12 is a spectrum taken under these conditions. Although no dissociation was evident, no quantitative data could be gained from this test, since a deterioration in electron multiplier gain had occurred between tests.

7.3 FURTHER INVESTIGATIONS

The results discussed in Section 7.2 were obtained for one orifice diameter, no second orifice, one axial location of the quadrupole detector head with respect to the orifice, one intended value of electron energy, one emission current, and one stagnation condition in the arc heater. In addition, only the mass range m/e = 1 to 50 has been observed. Future tests must be designed to evaluate the effects of changes in these physical and electrical degrees of freedom.

Before reliable quantitative interpretations of sampled spectra can be made, the effects of probe orifice diameter, quadrupole detector head location within the probe, and second orifice diameter must be investigated, especially with respect to their possible influence on the flow sample. With an apparently conservatively designed cryopump, it would be possible to

increase the sampled mass flow, since probe heating imposes a much more severe limitation on run time than does cryopumping time. With greater abundances sampled, better signal-to-noise ratios can be obtained, improving resolution.

Dissociation by the ionization process has been avoided in the electron-impact ionizer by selecting an electron energy voltage and a filament emission current of only one-third of their available maximums of 90 v and 1 ma, respectively. Many small-abundance species are detectable with greater electron energy, but with the concomitant sacrifice of induced dissociation of the more abundant species. A thorough species search should be made, however, in tests conducted with various electron and ion energy values.

The finite rate expansions described in Ref. 2 predict the appearance of a significant abundance of atomic oxygen at a stagnation temperature of only 10 to 15 percent higher than the nominal 3000°K condition selected for the tests described herein. Attempts to detect all such flow-induced atomic and ionized species should certainly be made.

SECTION VIII
SUMMARY

A probe for the sampling and instantaneous mass spectrometric analysis of a rarefied, high enthalpy, hypersonic flow has been designed, fabricated, and operated. It has been shown possible, with an LH_2 cryopump within the probe, both to establish the high vacuum environment within the probe required for proper operation of a quadrupole mass spectrometer, and to maintain the rarefied environment for sampling periods of at least 5 min in an arc-heated airflow of the following conditions: a stagnation condition of 3000°K and 10 atm; a nozzle exit static temperature and pressure of 80°K and 1.7×10^{-2} torr, respectively; a Mach number of approximately 14, with Re ≈ 4280 cm^{-1}.

Initial flow analyses correlated well with a nonequilibrium flow expansion calculation, even though several refinements of both empirical and analytical methods were yet to be made. The probe apparently successfully (1) admitted, without aerodynamic compression, a sample of the flow to its interior, where (2) a pressure of 10^{-6} to 10^{-4} torr was established and maintained for at least 5 min, and (3) performed without sustaining distortion or damage attributable to the hostile environment.

To complete development of the probe, the effects of changes in several physical and electrical parameters associated with both the probe itself and its mass spectrometer detecting head must be determined and evaluated. Extension of the test environment conditions to higher stagnation enthalpies must also be included in future test programs, to more accurately determine both the detectability limits and repeatability of the mass spectrometer output.

REFERENCES

1. Zonars, D. "Nonequilibrium Regime of Airflows in Contoured Nozzles: Theory and Experiments." AIAA Journal, Vol. 5, No. 1, January 1967, pp. 57-63.

2. MacDermott, W. N., and Marshall, J. C. "Nonequilibrium Nozzle Expansions of Partially Dissociated Air: A Comparison of Theory and Electron-Beam Measurements." AEDC-TR-69-66 (To be published)

3. Reddy, N. M. "The Use of Self-Calibrating Catalytic Probes to Measure Free-Stream Atom Concentration in a Hypersonic Flow." UTIAS Report 121, November 1966.

4. Bartz, J. A. "Heat Transfer Measurements with a Catalytic Flat Plate in a Nonequilibrium Expansion of Oxygen." AEDC-TR-67-249 (AD661985), November 1967.

5. Davis, F. H. "A Review of Physiochemical Methods of Nitrogen, Oxygen, and Nitric Oxide Measurements." AFFDL-TR-66-71, August 1966.

6. McLachlan, N. Theory and Application of Mathieu Functions, Oxford Press, 1947.

7. Paul, W., Reinhard, H., and von Zahn, V. Z. Physik, Vol. 152, No. 2, 1958, p. 143.

8. Rice, P. "Quadrupole Mass Spectrometers." Interim Report No. 2, Stanford Research Institute, 1962.

9. Scott, R. B. Cryogenic Engineering. D. Van Nostrand Company, Princeton, N. J., 1959.

10. MacDermott, W. N., Dix, R. E., and Shirley, B. H. "Low Density Boundary Layer Control by Liquid Hydrogen Cryopumping." AEDC-TR-65-148 (AD467446), August 1965.

11. MacDermott, W. N., Dix, R. E., and Shepard, J. E. "High Temperature, Low Density Boundary-Layer Control by Cryogenic Pumping." AEDC-TR-66-177 (AD634963), December 1966.

12. Patterson, G. N. Molecular Flow of Gases. John Wiley and Sons, New York, 1956, p. 92.

13. Hilsenrath, J. and Klein, M. "Tables of Thermodynamic Properties of Air in Chemical Equilibrium Including Second Virial Corrections from 1500°K to 15,000°K." AEDC-TR-65-58 (AD612301), March 1965.

14. Haygood, J. D., and Dawson, J. P. "Considerations in the Measurement of Cryopumping Capture Coefficients." AEDC-TR-65-68 (AD461132), April 1965.

15. Heald, J. H., Jr., and Brown, R. F. "Measurements of Condensation and Evaporation of Carbon Dioxide, Nitrogen, and Argon at Cryogenic Temperatures Using a Molecular Beam." AEDC-TR-68-110 (AD674596), September 1968.

16. Chuan, R. L. "A Study of the Condensation of Nitrogen below the Triple Point." USCEC R 56-201 (AD115052), February 1957.

APPENDIXES

STABLE TRAJECTORY

OUTPUT SIGNAL TERMINAL

UNSTABLE TRAJECTORY

$-(V_{DC} + V_0 \cos \omega t)$

GROUND APERTURE

FOCUS APERTURE

FARADAY CAGE

ELECTRON EXTRACTOR

SAMPLE FLOW

FILAMENT

IONIZER

ELECTRON MULTIPLIER

QUADRUPOLE FILTER

$+(V_{DC} + V_0 \cos \omega t)$
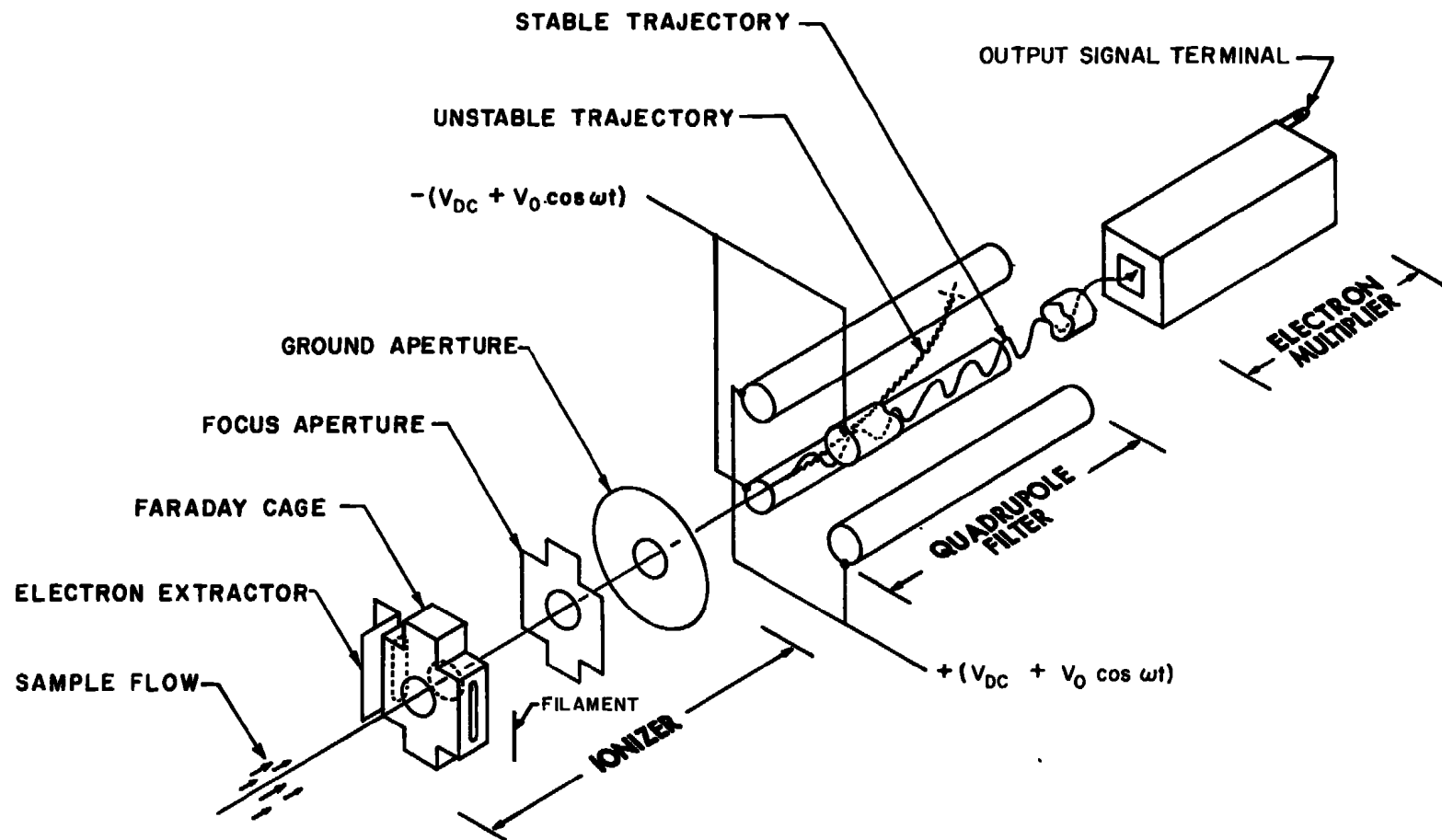
Fig. 1 Schematic of Quadrupole Mass Spectrometer

TEST CHAMBER

6-STAGE STEAM EJECTOR

HEAT EXCHANGER

REMOVABLE
DIFFUSER
SECTIONS

DIFFUSER

ARC HEATER
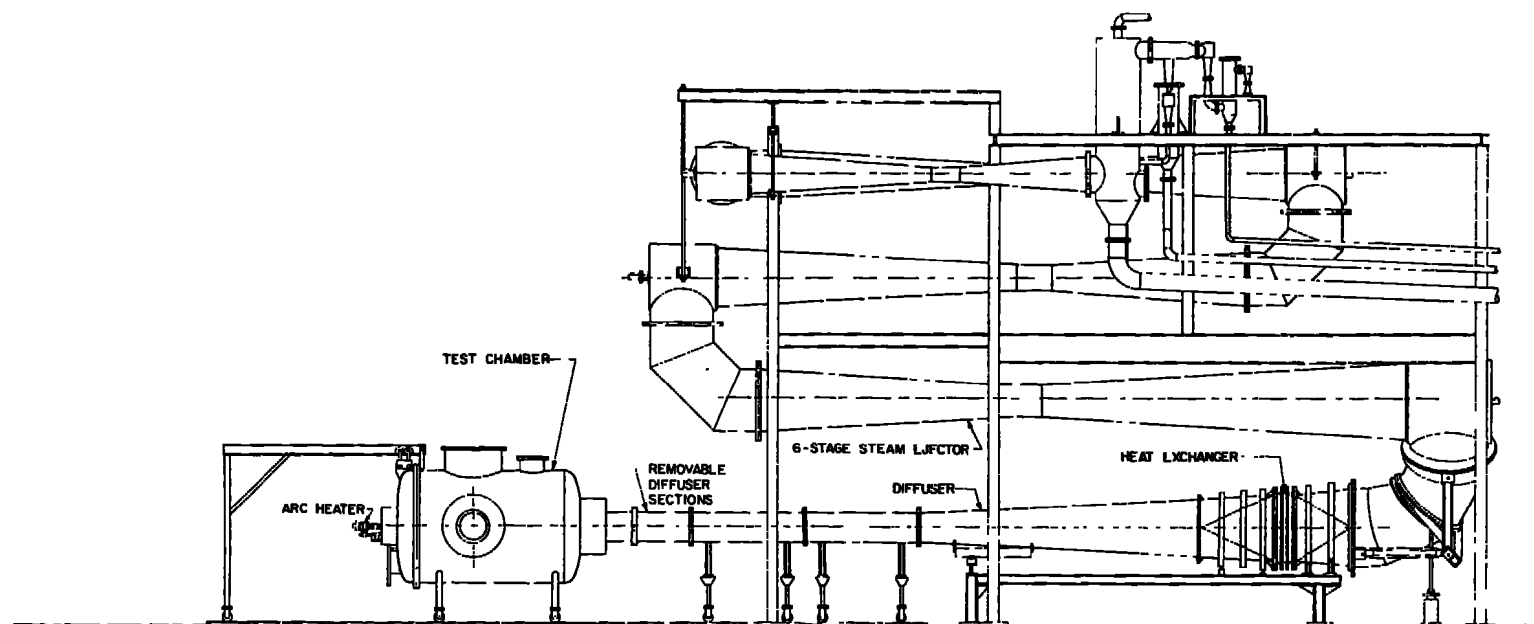
Fig. 2 Elevation of the 18-In. Wind Tunnel
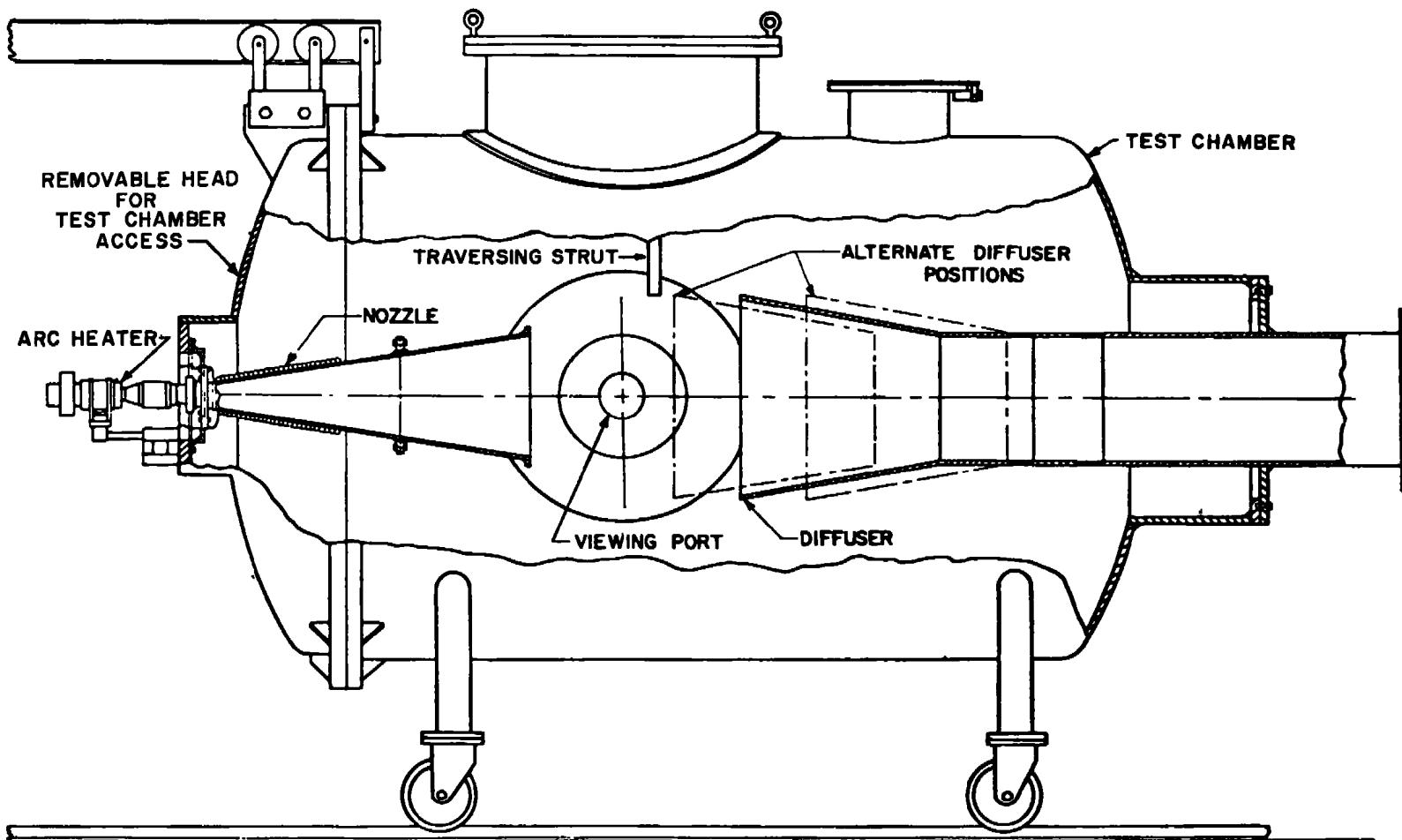
Fig. 3 Section View of the 18-In. Wind Tunnel Test Chamber
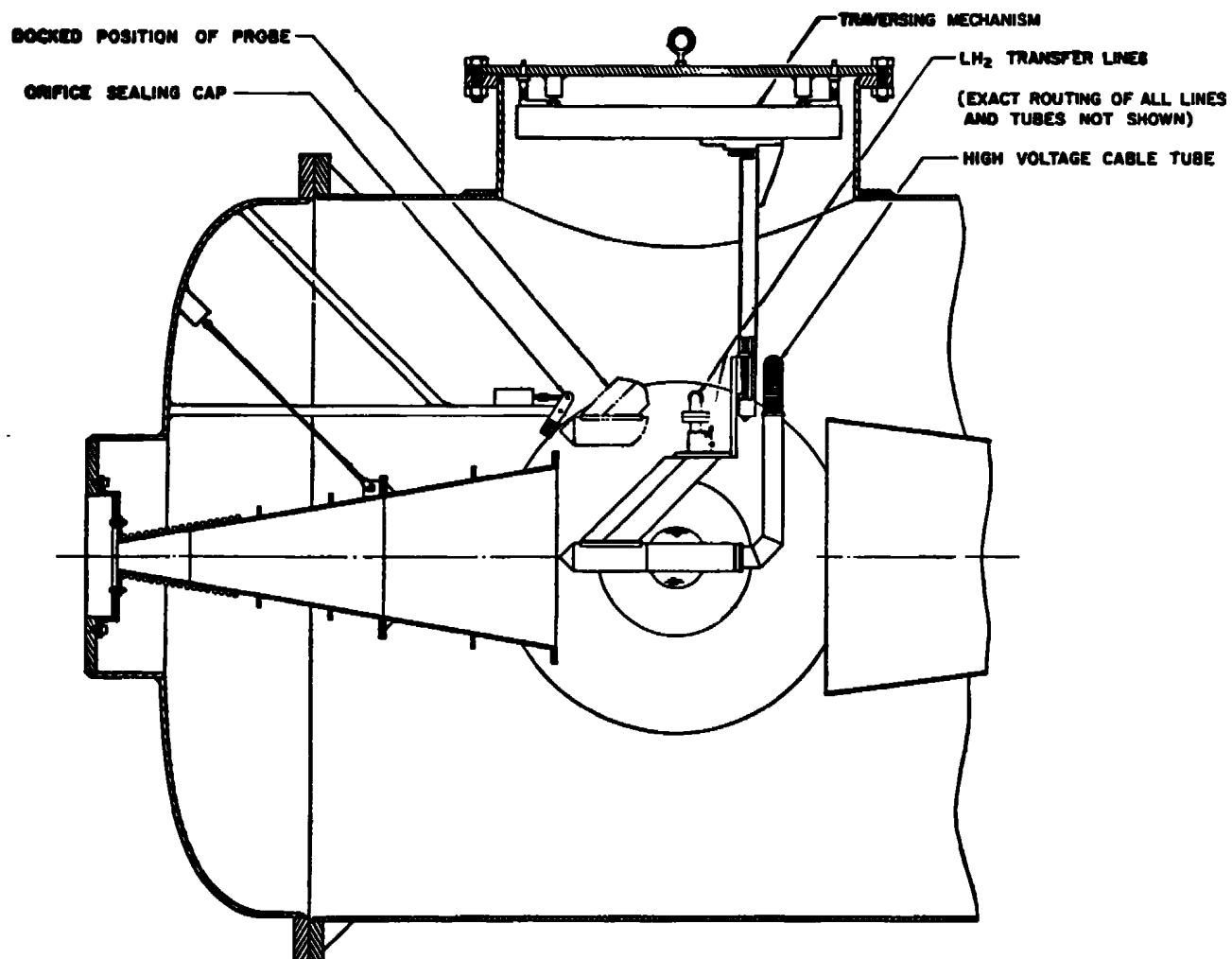
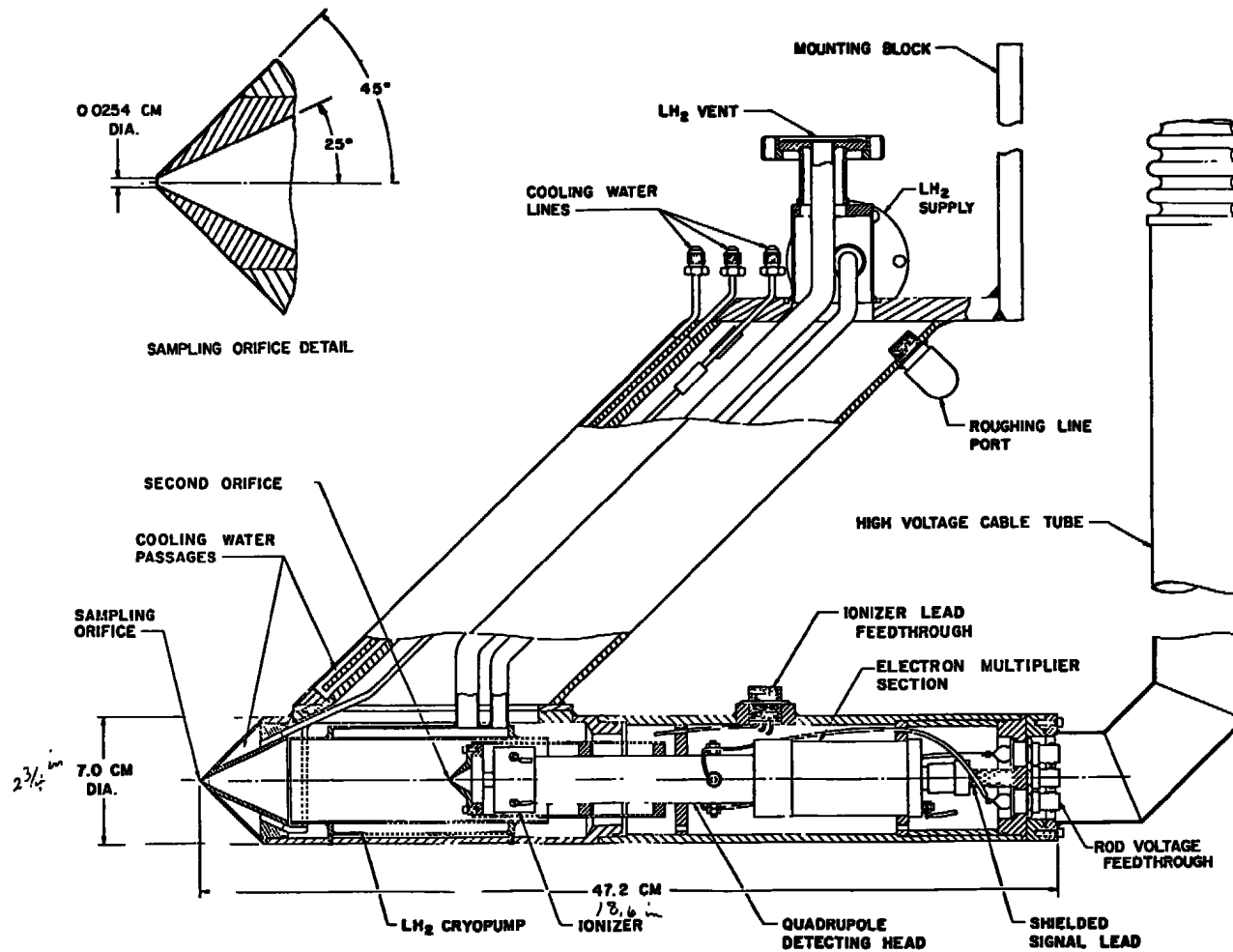Fig. 4 Sampling Probe Mounted in Test Section

SAMPLING ORIFICE DETAIL

0 0254 CM DIA.
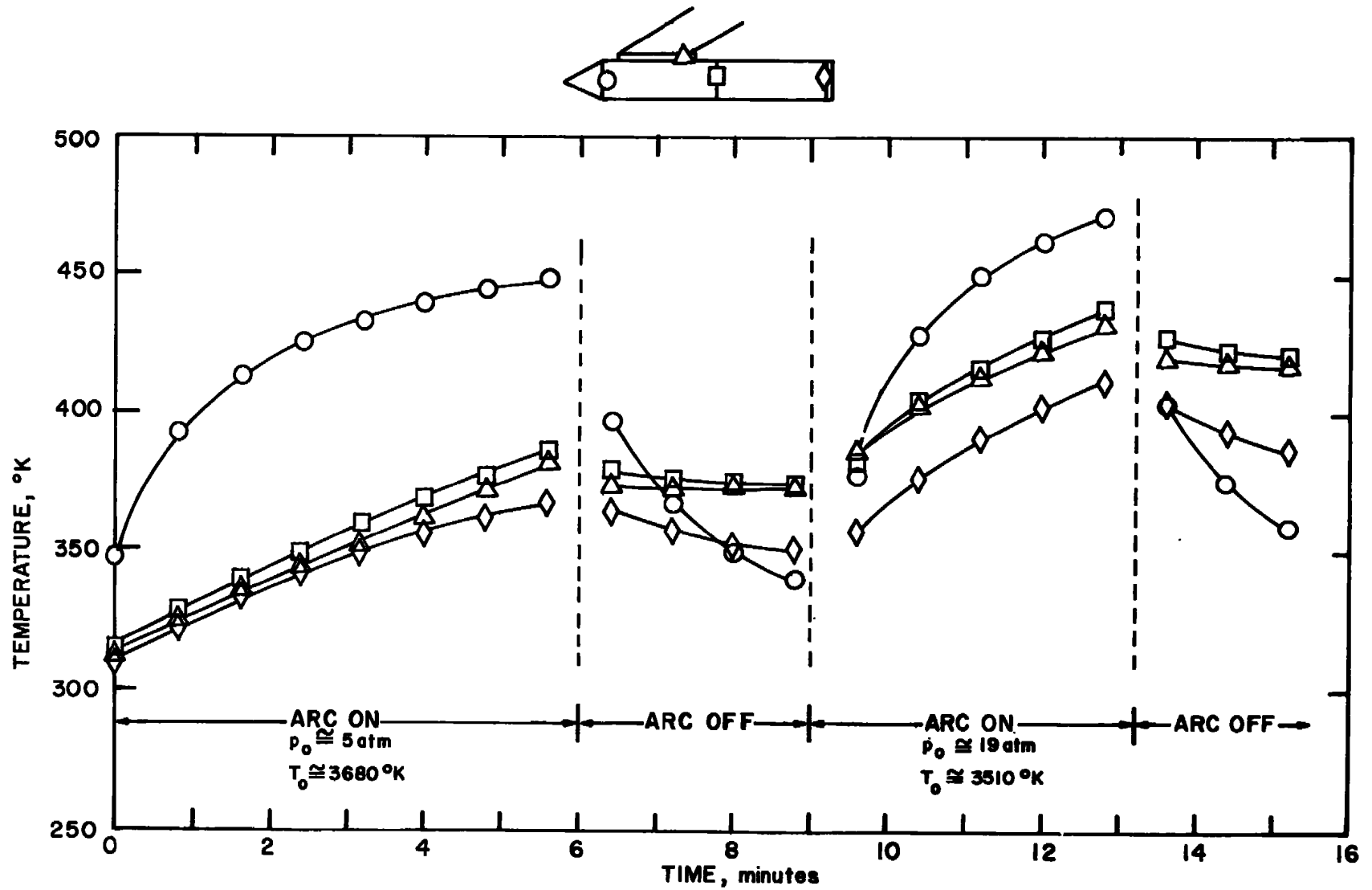
45°

25°

MOUNTING BLOCK

LH₂ VENT

COOLING WATER LINES

LH₂ SUPPLY

ROUGHING LINE PORT

SECOND ORIFICE

HIGH VOLTAGE CABLE TUBE

COOLING WATER PASSAGES

SAMPLING ORIFICE

IONIZER LEAD FEEDTHROUGH

ELECTRON MULTIPLIER SECTION

2³/₄ in

7.0 CM DIA.

ROD VOLTAGE FEEDTHROUGH

47.2 CM

18.6 in

LH₂ CRYOPUMP

IONIZER

QUADRUPOLE DETECTING HEAD

SHIELDED SIGNAL LEAD

Fig. 5 Section View of Sampling Probe

Fig. 6 Probe Heating Calibration
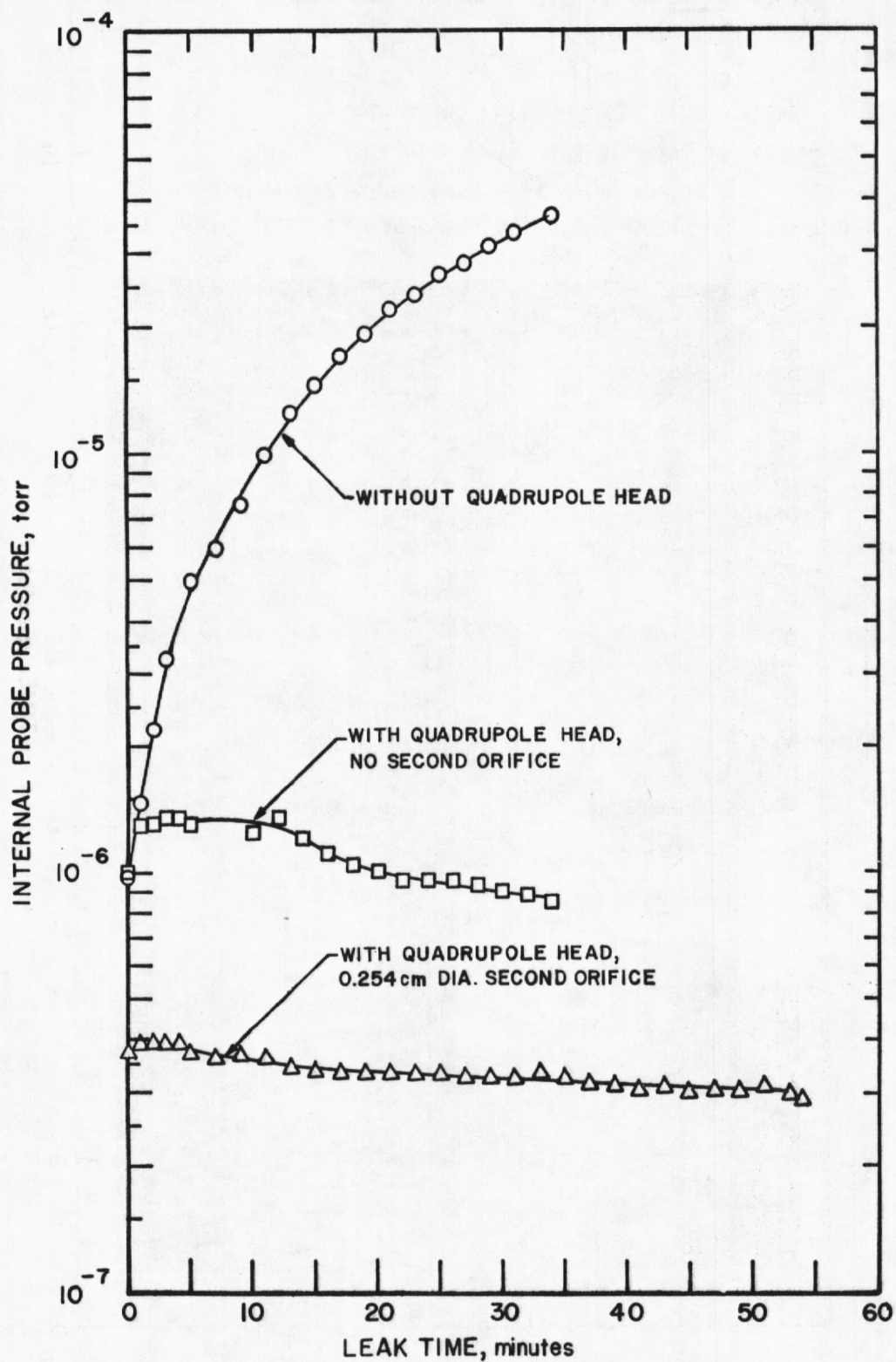
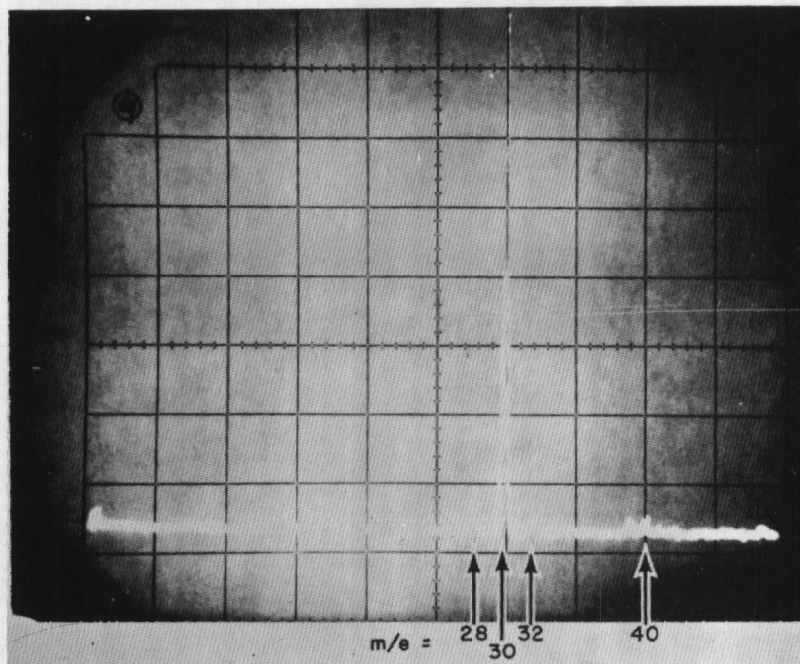Fig. 7 Probe Internal Pressure Calibration

FLOW CONDITIONS:

$p_0 = 9.3$ atm

$T_0 = 3130\ °K$

MASS SPECTROMETER SETTINGS:

Ion Energy = $+15\,v$

Electron Energy = 30 v Below Ion Energy

Filament Emission Current = 2×10^{-4} amp

a. Probe on Nozzle Centerline
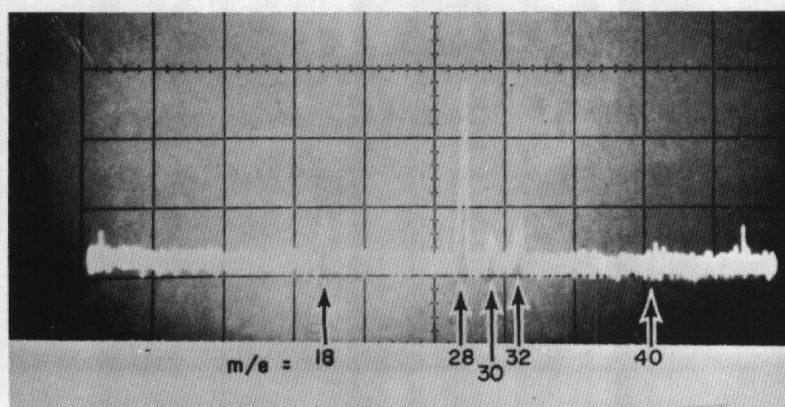
b. Probe in Nozzle Boundary Layer

Fig. 8 Initial Flow Spectra, m/e = 1 to 50

FLOW CONDITIONS:

$P_0 = 9.8$ atm

$T_0 = 3080$ °K

MASS SPECTROMETER SETTINGS:

Ion Energy = $+15$ v

Electron Energy = 30 v Below Ion Energy

Filament Emission Current = 2×10^{-4} amp
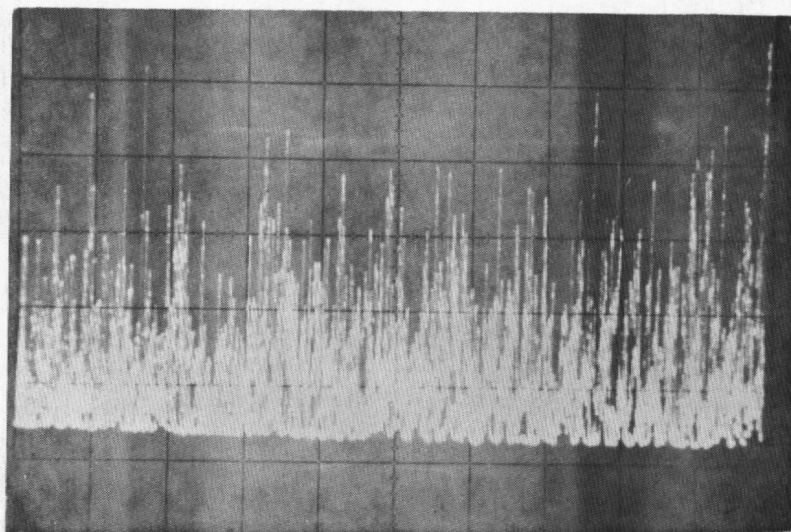

Fig. 9 Abundance of NO versus Time with Faraday Cage
Potential = 15 v

FLOW CONDITIONS:

   p_0 = 9.9 atm
   T_0 = 3100 °K
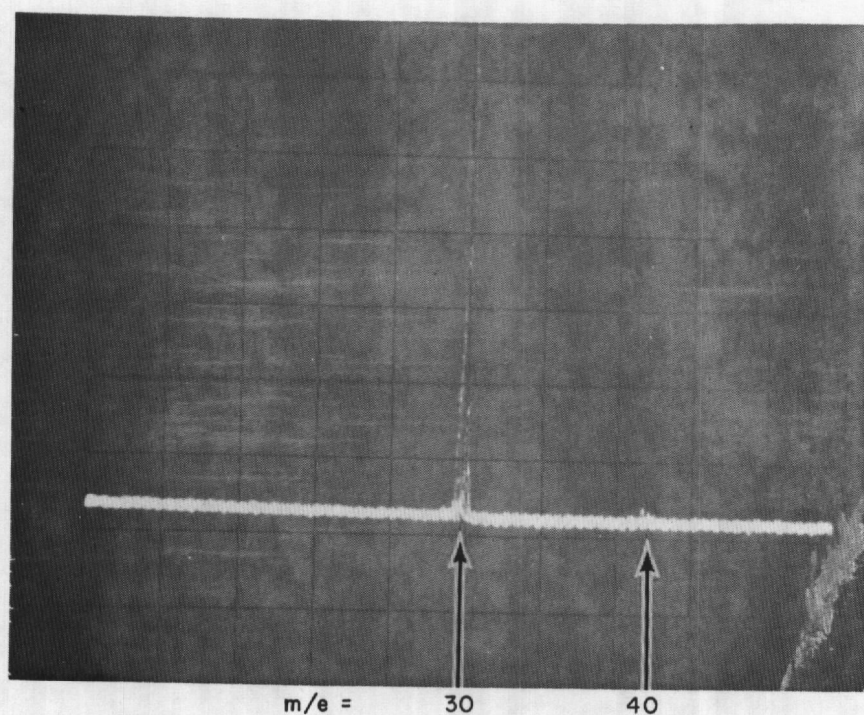
MASS SPECTROMETER SETTINGS:

   Ion Energy = 0 v
   Electron Energy = 30v Below Ion Energy
   Filament Off

m/e =   30   40

Fig. 10 Flow Spectrum with Faraday Cage Grounded,
m/e = 10 to 50

FLOW CONDITIONS:

   p_0 = 9.8 atm

   T_0 = 3080 °K

MASS SPECTROMETER SETTINGS:

   Ion Energy = + 105 v

   Effective Electron Energy = 135 v Below Ion Energy

   Filament Emission Current = 2×10^{-4} amp

m/e =   14 16 18   28 30 32   40
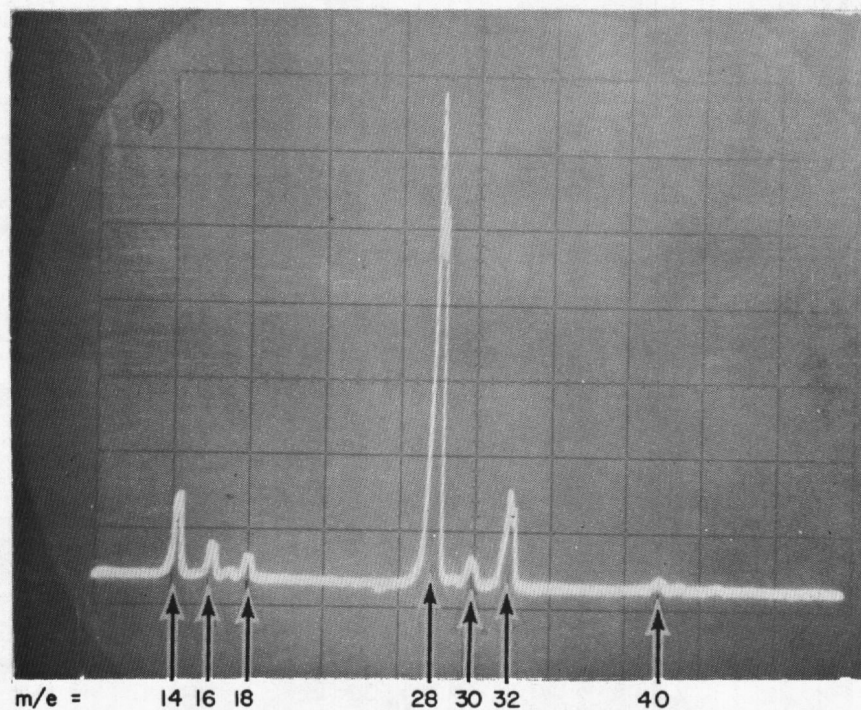
Fig. 11 Flow Spectrum with NO$^+$ Repelled, but with High
Electron Energy, m/e = 10 to 50

FLOW CONDITIONS:

    p_o = 10.0 atm
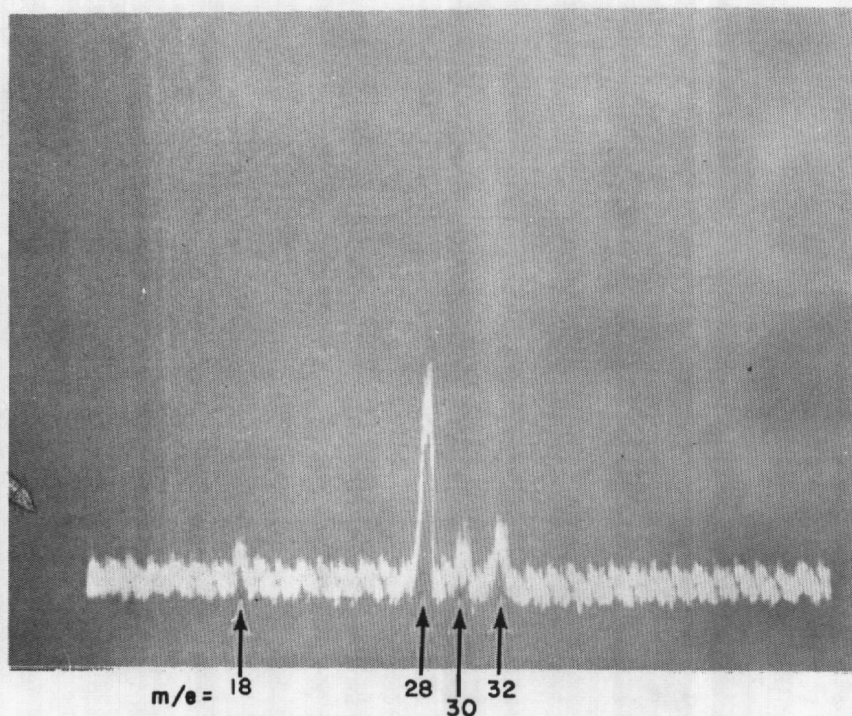
    T_o = 2920 °K

MASS SPECTROMETER SETTINGS:

    Ion Energy = 75v

    Electron Energy = 30v Below Ion Energy

    Filament Emission Current = 2×10^{-4} amp

Fig. 12 Flow Spectrum with NO^+ Repelled, and with Low
Electron Energy, m/e = 10 to 50

APPENDIX II
ESTIMATION OF REQUIRED CRYOSURFACE
AREA AND AVAILABLE PUMPING TIME

It was recognized that the probe orifice diameter would have a small value, probably approaching one mean free path of the free stream. However, to ensure a conservative estimate of required cryosurface area, continuum regime flow was assumed. Therefore, the volume flow rate to be cryopumped was computed from

$$\dot{V}_{cp} = \frac{\dot{m}_o}{\rho_{gcp}} = \frac{P_s \, A_o \, V_\infty \, T_{gcp}}{T_s \, P_{gcp}} \qquad (II-1)$$

Values of the gas properties at the cryopump could only be estimated, since the extent of thermal accommodation made by the sampled particles upon impact with items inside the probe before contacting the cryosurface was unknown. Using the design flow condition mentioned in Section 3.1, and assuming values of gas temperature and pressure at the cryosurface of 340°K and 10^{-5} torr, Eq. (II-1) yielded

$$\dot{V}_{cp} \approx (2.78 \times 10^9) \, A_o \, \frac{cm^3}{sec} \qquad (II-2)$$

Since it was required that the environment within the probe be substantially free of collisions, the free-molecular maximum specific pumping speed of the 20°K cryosurface was estimated from

$$S_{max} = \sqrt{\frac{\mathcal{R} \, T_{gcp}}{2\pi \, M}} \qquad (II-3)$$

which is derived in Ref. 14. Equation (II-3) assumed that all molecules striking the surface would be immediately immobilized - probably not at all true in the practical situation under consideration, hence a fractional capture coefficient of 0.9 was assumed. The value 0.9 was taken somewhat arbitrarily, since no data for cryopumping air on 20°K surfaces were available, yet it was in agreement both with published results from tests using room-temperature N_2, A, and CO_2 (Ref. 15), and not yet published results of tests in the same laboratory extending the gas temperatures to more than 2000°K. Then, Eq. (II-3) became

$$S_{eff} \approx 0.9 \sqrt{\frac{\mathcal{R} \, T_{gcp}}{2\pi \, M}} \qquad (II-4)$$

or, for air at 340°K

$$S_{eff} \approx 1.12 \times 10^4 \, \frac{cm^3}{sec\text{-}cm^2} \qquad (II-5)$$

The required cryosurface area was then defined by the quotient

$$A_{cp} = \frac{\dot{v}_{cp}}{S_{eff}} \approx \frac{(2.74 \times 10^9) \, A_o}{(1.12 \times 10^4)} \approx 2.48 \times 10^5 \, A_o \, \text{cm}^2 \qquad \text{(II-6)}$$

An estimate of the period of time during which the cryopump would function properly was made, using the method of Ref. 16. The expression for cryopumping time was derived from the assumption that an increasing cryodeposit surface temperature could be treated as a one-dimensional heat conduction process with a time-dependent boundary condition at the cryodeposit-gas interface. It was assumed that the cryosurface temperature was constant, and that the interface temperature was the saturation temperature of the gas. Useful cryopumping time, then, was

$$t_c = \frac{k \, \rho_c \, c(T_{sat} - T_{cp})^2 \, \exp(-2 \, \delta^2)}{F^2(\delta) \, \pi \, (\dot{q}_{cp})^2} \qquad \text{(II-7)}$$

where

$$\delta = 62.5 \, \bar{q}_s \sqrt{\frac{c}{k \, \rho_c}} \qquad \text{(II-8)}$$

where

$$\bar{q}_s = \frac{k(T_{sat} - T_{cp})}{\ell \, y_c} \qquad \text{(II-9)}$$

and

$$F(\delta) = \frac{2}{\pi} \int_o^\delta \exp(-\delta^2) \, d\delta \qquad \text{(II-10)}$$

Assigning the values $c = 0.39 \, \frac{\text{cal}}{\text{gm-}^\circ\text{K}}$, $k = 4 \times 10^{-4} \frac{\text{cal}}{\text{sec-cm-}^\circ\text{K}}$, $\rho_c = 1.0 \, \frac{\text{gm}}{\text{cm}^3}$, and $\ell = 60 \, \frac{\text{cal}}{\text{gm}}$ (all from Ref. 6), and $T_{sat} = 40^\circ\text{K}$, $T_{cp} = 20^\circ\text{K}$, and $y_c = 1$ cm, the values $\delta \approx 0.26$ and $f(\delta) \approx 0.29$ were computed.

Estimation of the heat flux per unit area of the cryosurface, $\dot{q}_{cp}$, proceeded from the assumption that the cryosurface would absorb both the stagnation enthalpy and the latent heat of solidification of the mass flow into the probe. The stagnation enthalpy for the design condition was approximately 1160 cal/gm, and the latent heat of solidification was taken as 60 cal/gm. The mass flow into the probe, again from a conservative assumption of continuum flow, was approximately 1.9×10^{-5} gm/sec. Therefore, $q_{cp} \approx 1.65 \times 10^{-4}$ cal/sec-cm^2.

Substituting into Eq. (7), $t_c \approx 8 \times 10^6$ sec. Without reliable values of the thermal and physical properties of air cryodeposits (c, k, and ρ), it was impossible to judge the credibility of t_{cp}. However, since the computed available cryopumping time was four orders of magnitude greater than the desired test time, it was concluded that fairly large unfavorable errors in the parameters affecting t_{cp} would still not show cryopumping time to be critical.

DOCUMENT CONTROL DATA - R & D

(Security classification of title, body of abstract and indexing annotation must be entered when the overall report is classified)

1. ORIGINATING ACTIVITY *(Corporate author)*	2a. REPORT SECURITY CLASSIFICATION
Arnold Engineering Development Center ARO, Inc., Operating Contractor Arnold Air Force Station, Tennessee 37389	UNCLASSIFIED
	2b. GROUP N/A

3. REPORT TITLE

SAMPLING PROBE FOR INSTANTANEOUS MASS SPECTROMETRIC ANALYSIS OF RAREFIED HIGH ENTHALPY FLOW

4 DESCRIPTIVE NOTES *(Type of report and inclusive dates)*
Final Report   July 1, 1966 to September 30, 1968

5. AUTHOR(S) *(First name, middle initial, last name)*
R. E. Dix, ARO, Inc.

6. REPORT DATE	7a. TOTAL NO. OF PAGES	7b. NO. OF REFS
April 1969	42	16

8a. CONTRACT OR GRANT NO. F40600-69-C-0001	9a. ORIGINATOR'S REPORT NUMBER(S)
b. PROJECT NO. 4344	AEDC-TR-69-37
c. Program Element 65701F	9b. OTHER REPORT NO(S) *(Any other numbers that may be assigned this report)*
d. Task 02	N/A

10. DISTRIBUTION STATEMENT

This document has been approved for public release and sale; its distribution is unlimited.

11. SUPPLEMENTARY NOTES	12. SPONSORING MILITARY ACTIVITY
Available in DDC.	Arnold Engineering Development Center, Air Force Systems Command, Arnold AFS, Tennessee 37389

13. ABSTRACT

An aerodynamically shaped probe has been developed for instantaneous mass spectrometric analyses of gas samples taken from low density, high enthalpy, hypersonic flows. The requisite 10^{-5} torr operating pressure for a quadrupole mass spectrometer mounted in the water-cooled probe was established and maintained by a liquid-hydrogen cryopump. During an initial series of 5-min tests, the detected composition of an arc-heated airflow with a stagnation condition of approximately 10 atm at $3000°K$ agreed well with a nonequilibrium flow expansion calculation.

DD FORM 1473
1 NOV 65

14. KEY WORDS	LINK A		LINK B		LINK C	
	ROLE	WT	ROLE	WT	ROLE	WT
mass spectrometers						
probes						
high enthalpy flow						
gas analysis						
hypersonic flow						
wind tunnel tests						

AFSC
Arnold AFS Tenn